AGU PUBLICATIONS

Water Resources Research

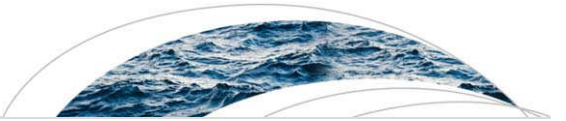

RESEARCH ARTICLE

10.1002/2014WR016443

Key Points:
- Soil water content was determined accurately with cosmic ray probes
- An empirical linear correction for variable aboveground biomass was developed
- The COSMIC operator, N_0 and the hmf method were used for evaluation

Correspondence to:
R. Baatz,
r.baatz@fz-juelich.de

Citation:
Baatz, R., H. R. Bogena, H.-J. Hendricks Franssen, J. A. Huisman, C. Montzka, and H. Vereecken (2015), An empirical vegetation correction for soil water content quantification using cosmic ray probes, *Water Resour. Res.*, *51*, 2030–2046, doi:10.1002/2014WR016443.

Received 21 SEP 2014
Accepted 24 FEB 2015
Accepted article online 10 MAR 2015
Published online 8 APR 2015

An empirical vegetation correction for soil water content quantification using cosmic ray probes

R. Baatz[1], H. R. Bogena[1], H.-J. Hendricks Franssen[1], J. A. Huisman[1], C. Montzka[1], and H. Vereecken[1]

[1]Agrosphere (IBG-3), Forschungszentrum Jülich GmbH, Jülich, Germany

Abstract Cosmic ray probes are an emerging technology to continuously monitor soil water content at a scale significant to land surface processes. However, the application of this method is hampered by its susceptibility to the presence of aboveground biomass. Here we present a simple empirical framework to account for moderation of fast neutrons by aboveground biomass in the calibration. The method extends the N_0-calibration function and was developed using an extensive data set from a network of 10 cosmic ray probes located in the Rur catchment, Germany. The results suggest a 0.9% reduction in fast neutron intensity per 1 kg of dry aboveground biomass per m^2 or per 2 kg of biomass water equivalent per m^2. We successfully tested the novel vegetation correction using temporary cosmic ray probe measurements along a strong gradient in biomass due to deforestation, and using the COSMIC, and the hmf method as independent soil water content retrieval algorithms. The extended N_0-calibration function was able to explain 95% of the overall variability in fast neutron intensity.

1. Introduction

Hydrologic processes at the land surface are strongly influenced by surface soil water content because it controls water availability for transpiration, evaporation, and groundwater recharge [*Brutsaert*, 2005]. Soil water content measurements are therefore a valuable source of information for hydrologic [*Brocca et al.*, 2012], land surface [*Jung et al.*, 2010], and atmospheric circulation models [*Koster et al.*, 2004]. The wealth of available soil water content measurement techniques at various temporal and spatial scales has extensively been reviewed [e.g., *Robinson et al.*, 2008; *Vereecken et al.*, 2008, 2014]. Among these techniques, cosmic ray probes (CRPs) are an emerging technology to determine soil water content from passive neutron counting [*Zreda et al.*, 2008]. This new technique addresses the need for continuous soil water content measurements at the horizontal scale of several tens of ha. The method utilizes the fact that hydrogen moderates secondary cosmic ray neutrons much more effectively than other atoms present in the soil. There are two main reasons for this. First, hydrogen nuclei have a similar mass as fast neutrons and thus fewer fast neutron-hydrogen nuclei collisions are needed to slow down a fast neutron to the thermal level. Second, hydrogen has the highest elastic scattering cross section of the most abundant elements in the soil [*Zreda et al.*, 2012]. This results in an inverse relationship between the abundance of hydrogen atoms near the soil surface and secondary cosmic ray intensity or neutron intensity [*Hendrick and Edge*, 1966]. Spatially averaged soil water content determined using in situ calibrated CRPs was found to be in good agreement with independently determined areal average soil water content at sites where biomass showed little variation over the year [*Baatz et al.*, 2014; *Bogena et al.*, 2013; *Desilets et al.*, 2010; *Franz et al.*, 2012a; *Zreda et al.*, 2008]. However, it was also shown that aboveground biomass within the CRP footprint reduced measured fast neutron intensity due to the moderating power of hydrogen contained in vegetation water and plant tissue [*Coopersmith et al.*, 2014; *McJannet et al.*, 2014]. Hence, dynamic changes in aboveground biomass were shown to affect the CRP counting rate and thus the accuracy of the soil water content measurements [*Franz et al.*, 2013c; *Villarreyes et al.*, 2011].

At present, three methods of different complexity exist to convert measured neutron intensity into soil water content: the N_0 method [*Desilets et al.*, 2010], the hydrogen molar fraction method (hmf method) [*Franz et al.*, 2013b], and the COSMIC operator [*Shuttleworth et al.*, 2013]. These methods were recently compared and evaluated by *Baatz et al.* [2014]. Of these methods, only the hmf method explicitly accounts for additional hydrogen contained in aboveground biomass. However, it is limited by a maximum hydrogen

molar fraction of 0.23 moles moles^{-1} that corresponds with liquid water. Several studies have shown that this maximum hydrogen molar fraction can be exceeded in the case of high aboveground biomass [*Baatz et al*., 2014; *Franz et al*., 2013b]. Moreover, numerical experiments with a neutron interaction model demonstrated that hydrogen contained in forest trees cannot simply be conceptualized as an additional layer of water on top of the soil [*Franz et al*., 2013c]. Instead, these simulations indicated that the impact of aboveground biomass on neutron moderation depends on forest structure and tree geometry (e.g., tree spacing, tree trunk diameter, etc.).

In principle, neutron interaction models [e.g., *Pelowitz*, 2005] are viable tools to develop correction functions to account for biomass effects on soil water content estimates derived from CRPs. However, the accuracy of such physically based modeling of neutron interactions with biomass is limited by the complexity of accurately representing and parameterizing total above and belowground biomass, which depends on plant species and generally is strongly heterogeneous [*Franz et al*., 2013c]. In addition, such simulations are computationally intensive and thus unfavorable for practical applications of the CRP method.

Here we aim to develop a simple empirical framework to account for aboveground biomass effects on fast neutron moderation. Such a correction method for biomass would enhance the functionality of the N_0 method and the COSMIC operator by eliminating the need for in situ calibration when dry aboveground biomass is known or can be estimated with reasonable accuracy. In addition, such a correction for biomass would enable CRP applications in locations with strong changes in aboveground biomass and the use of mobile CRP surveys [e.g., *Chrisman and Zreda*, 2013] in areas with strong spatial variation in aboveground biomass. To develop the empirical framework, we quantified the moderating effect of aboveground biomass at a range of sites with different environmental conditions by calibrating 10 permanent CRPs using soil sampling campaigns. Measured fast neutron intensity was corrected for air pressure, incoming cosmic ray intensity, atmospheric humidity, and sensor-specific counting efficiency. We evaluated the efficiency of the correction method for aboveground biomass using several different data sets acquired on sites with different amounts of aboveground biomass.

2. Materials and Methods

2.1. Site Description and Instrumentation

All measurements were made in the Rur catchment that covers an area of 2354 km^2 and is located at the western border of Germany (Figure 1). It is part of the Terrestrial Environmental Observatories (TERENO) infrastructure [*Bogena et al*., 2012; *Zacharias et al*., 2011]. Elevation ranges between 15 m in the lowland region in the north and 690 m in the low-mountainous Eifel region in the south. Mean annual precipitation increases from less than 600 mm in the north to 1400 mm in the south [*Montzka et al*., 2008]. The lower northern part of the catchment is dominated by crop land, while the low-mountainous part is dominated by grassland and forest.

We installed 10 permanent cosmic ray probes at a height of 1.5 m (CRS1000, HydroInnova LLC, 2009) in the Rur catchment (Figure 1). All 10 probes contain a moderated neutron counter that consists of a metal tube (3 cm in diameter and 30 cm in length) filled with high pressure ^{3}He gas mantled with polyethylene. Five of the CRPs contain a second bare neutron counter without polyethylene mantle. A high voltage is applied to both ends of the tubes, which triggers an ionization process that produces a charged cloud that is registered as a single count by the pulse module when a neutron passes through the ^{3}He tube. The network of CRPs has been operational since May 2012 and the CRP stations cover the main land use types of the Rur catchment: grassland (Rollesbroich, RollesbroichN, Kall, and Rur Aue), crop land (Aachen, Gevenich, Heinsberg, and Merzenhausen), and forest (Wildenrath and Wuestebach). Detailed information on altitude, mean annual precipitation and temperature, and land use fractions are presented in Table 1 for all sites.

Two sites with CRPs (Rollesbroich and Wuestebach) were additionally equipped with a wireless soil water content sensor network (SoilNet, Forschungszentrum Jülich GmbH) described by *Bogena et al*. [2010]. Soil water content sensors were installed in 5, 20, and 50 cm depth and provide soil water content estimates at 15 min intervals. Calibration and data analysis of the SoilNet installed in the Wuestebach catchment is described by *Bogena et al*. [2010] and *Rosenbaum et al*. [2012], whereas *Qu et al*. [2013] provide this information for the Rollesbroich test site. The use of SoilNet data for calibration and evaluation of soil water content derived from neutron intensity measurements is described in more detail by *Bogena et al*. [2013] and *Baatz et al*. [2014].

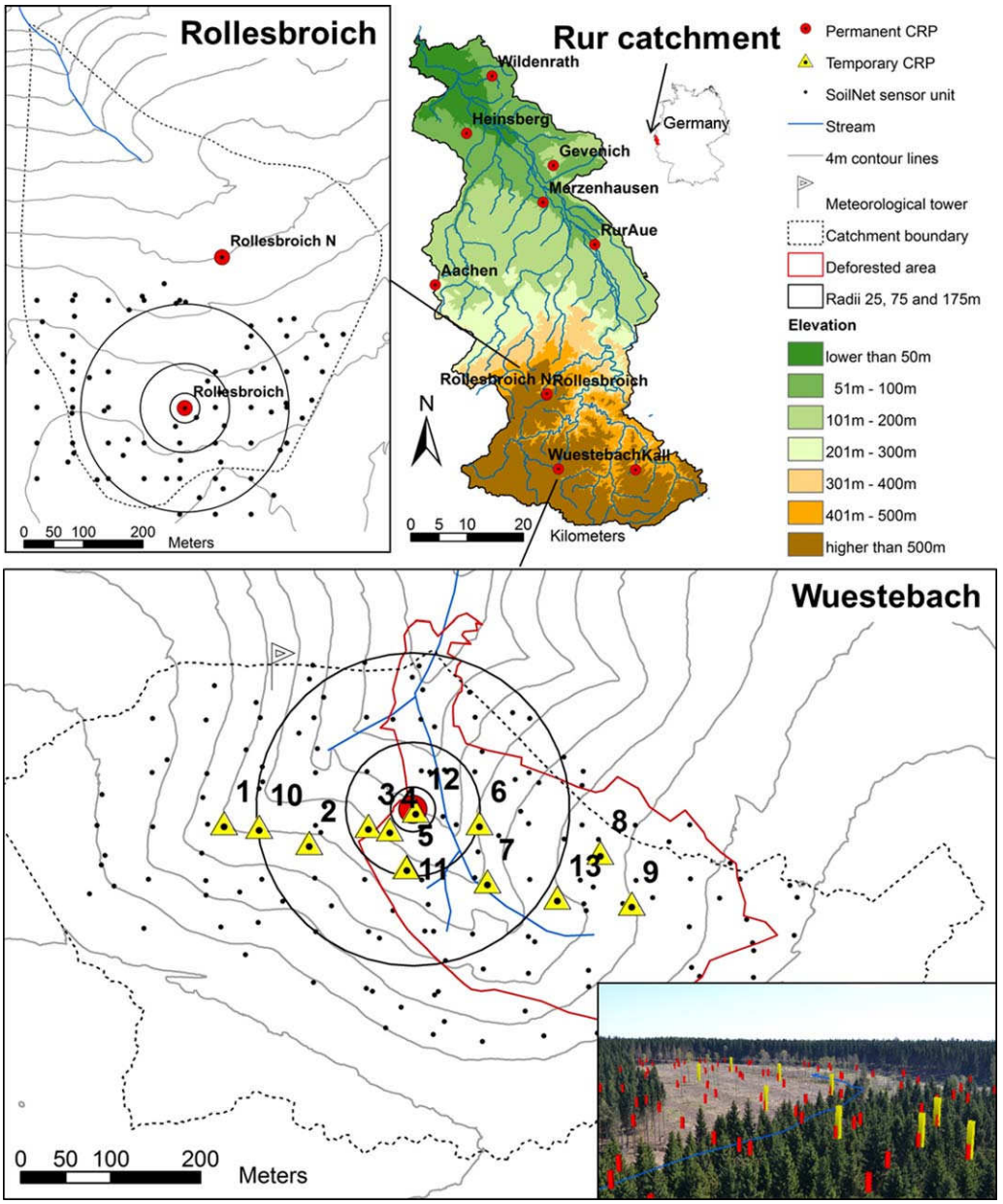

Figure 1. Locations of the 10 permanently installed CRPs in the Rur catchment (top right), the Rollesbroich test site equipped with an in situ soil water content sensor network (top left) and the Wuestebach test site with the temporary CRPs, the deforested area and radii used for calibration at 25, 75, and 175 m (bottom figure), and a photograph taken from the meteorological tower in 2014 with locations of in situ SoilNet nodes (red), 9 of 13 temporary CRPs (yellow), and the Wuestebach stream (bottom right).

As part of a deforestation experiment [*Bogena et al*., 2014], 9 ha of Norway Spruce trees were removed in August 2013 within a part of the Wuestebach catchment (Figure 1). The permanently installed CRP at Wuestebach was removed during the deforestation activities, and afterward reinstalled at the original location. Additionally, neutron intensity measurements for short periods (between 24 and 405 h) were taken at 13 locations at the Wuestebach test site from January to May 2014 (Figure 1). These locations were selected in such a way that the CRP footprint contained distinctly different amounts of aboveground biomass.

2.2. Derivation of Soil Water Content From CRP Measurements

2.2.1. Required Fast Neutron Intensity Corrections

The use of CRP measurements to determine soil water content requires a range of corrections of the measured neutron intensity. Large-scale networks of CRPs need to consider corrections associated with varying

Table 1. Site Characteristics of the 10 Permanent CRPs in the Rur Catchment (Annual Temperature, Annual Precipitation, Land Use Fractions Excluding Surface Water Bodies (<1%))

	Latitude	Longitude	Start of Measurement	Altitude (m asl)	T(av), °C	P (mm)	Land Use [%]			
							Grasses	Crops	Forest	Urban
Aachen	50.798550N	6.024716E	13 Jan 2012	232	9.94	952	19	72	0	9
Gevenich	50.989220N	6.323550E	7 Jul 2011	108	10.16	884	0	85	0	15
Heinsberg	51.041104N	6.104238E	9 Sep 2011	57	10.25	814	35	39	2	24
Kall	50.501332N	6.526450E	15 Sep 2011	504	7.71	935	72	11	0	17
Merzenhausen	50.930325N	6.297468E	19 May 2011	94	10.22	825	1	82	0	16
Rollesbroich	50.621911N	6.304241E	19 May 2011	515	7.88	1307	92	0	0	8
RollesbroichN	50.624190N	6.305142E	22 May 2012	506	7.91	1309	87	0	0	12
RurAue	50.862329N	6.427335E	8 Nov 2011	102	10.13	743	58	25	11	6
Wildenrath	51.132744N	6.169175E	7 May 2012	76	10.28	856	3	7	88	2
Wuestebach	50.503487N	6.333017E	1 Feb 2011	605	7.47	1401	7	0	93	0

cutoff rigidity [e.g., *Zreda et al*., 2012] but this is not required for the relatively small Rur catchment. In this study, we corrected measured fast neutron intensity to standard air pressure (1013 hPa), a reference level of incoming cosmic ray intensity, and zero air humidity using the procedures described by *Baatz et al*. [2014]. The corrected neutron intensity is denoted as N_{pih}

$$N_{pih}=N_{raw}\times\{exp(\beta\times(P-P_{ref}))\}\times\{I_{ref}/I\}\times\{1+0.0054\times(\rho_{wv}-\rho_{ref})\}, \quad (1)$$

where the term $\{exp(\beta\times(P-P_{ref}))\}$ describes the correction of air pressure P [hPa] at the time of measurement to a reference pressure $P_{ref}=1013$ hPa using the barometric pressure coefficient $\beta=0.0076$ hPa^{-1} [*Desilets and Zreda*, 2003], $\{I_{ref}/I\}$ describes the correction of incoming cosmic ray intensity I [counts per second] to a reference incoming cosmic ray intensity I_{ref} [counts per second] [*Zreda et al*., 2012] obtained from the Neutron Monitor Database (NMDB), and $\{1+0.0054\times(\rho_{wv}-\rho_{ref})\}$ describes the correction for atmospheric water content at 2 m height [g m^{-3}] to a reference atmospheric water content of $\rho_{ref}=0$ g m^{-3} [*Rosolem et al*., 2013].

This study also considers corrections for sensor-specific counting efficiency as introduced by *McJannet et al*. [2014]. Counting efficiency of a CRP may vary due to differences in the polyethylene shielding thickness or in the pressure of the Helium gas and should be considered to improve comparability between CRPs within a network. For this correction, a reference CRP with two moderated counters was placed next to each permanent CRP station for a period of at least 10 h. An efficiency scaling factor η_{ref} was determined for each CRP from these reference CRP measurements using

$$\eta_{Iref}=N_{ref}/N_i, \quad (2)$$

where N_{ref} [cph] is the mean raw neutron intensity of the reference CRP over the measurement interval and N_i [cph] is the corresponding mean neutron intensity of the CRP that requires correction for counting efficiency. The final corrected neutron intensity that also considers counting efficiency, N_{epih}, was then obtained using

$$N_{epih}=N_{pih}\times\eta_{ref}. \quad (3)$$

2.2.2. Support Volume of CRPs

The support volume of CRP measurements is often defined as the volume from which 86% of the fast neutrons originate [*Zreda et al*., 2008]. According to *Desilets and Zreda* [2013], the horizontal CRP footprint is approximately 300 m in radius at sea level, depending on air density, elevation, and air humidity. If soil moisture content within the CRP footprint follows a Gaussian random field model, the spatial variability of soil water content has a negligible impact on fast neutron intensity. In this case, the weighted horizontal average soil water content is measured by the CRP [*Franz et al*., 2013a]. The decrease in sensitivity with distance from the CRP needs to be considered when environmental factors that affect CRP measurements, such as soil water content and biomass, are heterogeneously distributed within the footprint. This can be achieved with the COSMOS calibration scheme [*Zreda et al*., 2012], which divides the horizontal footprint into three radii at 25, 75, and 175 m and proposes to take calibration measurements every 60° (i.e., six points). This results in a set of 18 calibration samples that can be arithmetically averaged to obtain the

mean properties within the footprint because of the appropriately chosen radii [*Zreda et al*., 2012]. A second approach for horizontal weighting was suggested by *Bogena et al*. [2013]. They used the cumulative fraction of counts in the horizontal footprint [*Zreda et al*., 2008] to calculate appropriate weighting factors for horizontal segments with increasing radii up to 300 m [*Franz et al*., 2013a].

The depth of the CRP support volume was investigated by *Franz et al*. [2012b] and ranges from 10 cm for moist soils up to 70 cm for dry silicate soils. We adopted the vertical weighting scheme developed by *Bogena et al*. [2013] to assign weights to vertical layers of soil water content. Similar to the exponential weighting used in the COSMIC operator [*Shuttleworth et al*., 2013], this scheme considers nonlinear weighting for the vertically heterogeneous soil water content distributions that are typically encountered in real-world conditions.

2.2.3. Conversion of Fast Neutron Intensity to Soil Water Content

We used three methods to convert neutron intensity to soil water content: (i) the N_0 method, (ii) the COSMIC operator, and (iii) the hmf method. The N_0 method allows direct conversion of measured fast neutron intensity (N_{epih}) to soil water content [*Desilets et al*., 2010] using

$$\theta_{grav} = \theta_{vol} \times \rho_{h2o}/\rho_{bd} = a_0 \times \left(N_{epih}/N_0 - a_1\right)^{-1} - a_2, \quad (4)$$

where $a_0 = 0.0808$, $a_1 = 0.372$, and $a_2 = 0.115$ are semiempirical parameters that are constant for all sites, N_0 is a site-dependent time-constant calibration parameter, θ_{grav} is the total gravimetric soil water content (soil water content plus lattice water in g g^{-1}) [*Zreda et al*., 2012], θ_{vol} is the total volumetric soil water content [cm^3 cm^{-3}], ρ_{h2o} is the density of water [g cm^{-3}], and ρ_{bd} is the dry soil bulk density [g cm^{-3}]. N_0 is determined using weighted mean total gravimetric soil water content and measured corrected neutron intensity over a short time interval.

The COSMIC operator was developed to use CRP measurements in data assimilation [*Shuttleworth et al*., 2013]. The conversion of the neutron signal into soil water content profiles by the COSMIC operator was analyzed in detail by *Rosolem et al*. [2014]. A recent evaluation by *Baatz et al*. [2014] showed that COSMIC can also be used to obtain accurate soil water content estimates from fast neutron intensity measurements. In this study, the COSMIC operator was parameterized with a site-specific mean bulk density (0–30 cm), high-energy neutron-soil interaction constants $L_1 = 162.0$ g cm^{-2} and $L_2 = 129.1$ g cm^{-2}, fast neutron-soil interaction constants $L_3 = -31.65 + 99.29 \times \rho_{bd}$ and $L_4 = 3.16$ g cm^{-2}, and an efficiency factor $\alpha = 0.404 - 0.101 \times \rho_{bd}$ for the relative efficiency to create fast neutrons. Like for the N_0 method, lattice water and soil water content make up the total soil water content. A site-specific calibration parameter N_{COSMIC} was determined using measured corrected neutron intensity and weighted mean total soil water content at the time of calibration.

The universal calibration function or hydrogen molar fraction method (hmf method) was developed to enable calibration of CRPs at locations where it is difficult to undertake in situ calibration measurements [*Franz et al*., 2013b]. The hydrogen molar fraction (hmf) is calculated with

$$hmf = \sum H / \sum E_{all}, \quad (5)$$

where $\sum H$ in mol is the sum of all moles of hydrogen within the CRP footprint and $\sum E_{all}$ in mol is the sum of all moles of all elements which include for simplicity air (NO), dry soil (SiO_2), soil carbon (C), and vegetation besides the sources of water and hydrogen (H_2O). In this simplified approach, vegetation consists of water and cellulose ($C_6H_{12}O_5$) only, and it was initially assumed that vegetation was present as a layer on top of the soil. Using the MCNPx code, *Franz et al*. [2013b] found a monotonic decreasing exponential relationship between neutron intensity and hmf

$$N_{epih}/N_s = a \times \exp\left(b \times hmf\right) + c \times \exp(d \times hmf), \quad (6)$$

where N_S is a universal calibration parameter and $a = 4.486$, $b = -48.1$, $c = 4.195$, and $d = -6.181$ are constants. *McJannet et al*. [2014] updated the parameters of equation (6) to $a = 3.007$, $b = -48.391$, $c = 3.499$, and $d = 5.396$ based on their calibration data and additional MCNPx simulations which assumed that CRPs measure an additional 30% of slow neutrons. We consider both parameterizations in the remainder of this study. Additional simulations and explicit modeling of tree trunks with the MCNPx code revealed that tree biomass cannot be simplified as a layer upon the soil as assumed in the derivation of hmf in equation (5)

Table 2. Results of the 16 Calibration Campaigns at the Permanent CRPs (Dry Soil Bulk Density (ρ_{bd}), Lattice Water (lw), Volumetric Water Content (θ_{vol}), Total Gravimetric Soil Water Content (θ_{grav}), CRP Efficiency Factor (η_{ref}), Biomass Water Equivalent (BWE), Dry Aboveground Biomass (AGB_{dry}), Corrected Fast Neutron Intensity (N_{epih}), and Calibration Parameters N_0, $N_{S,a}$ [after *Franz et al*., 2013b], and $N_{S,b}$ [after *McJannet et al*., 2014], and Efficiency of a Temporary CRP Used in the Wuestebach Experiment

Location	ρ_{bd} (g cm^{-3})	lw (cm^3 cm^{-3})	θ_{vol} (cm^3 cm^{-3})	θ_{grav} (g g^{-1})	η_{ref}	BWE (kg m^{-2})	AGB_{dry} (kg m^{-2})	N_{epih} (cph)	N_0 (cph)	$N_{S,a}$ (cph)	$N_{S,b}$ (cph)
Aachen	1.12	0.058	0.38	0.39	1.01	3.3	1.2	631	1188	485	501
Aachen	1.20	0.063	0.27	0.28	1.01	3.3	1.2	691	1194	474	497
Gevenich	1.31	0.034	0.26	0.22	0.97	3.7	1.4	744	1216	475	503
Gevenich	1.42	0.037	0.15	0.13	0.97	3.7	1.4	829	1181	431	469
Heinsberg	1.27	0.039	0.34	0.30	0.97	2.7	1.2	683	1203	477	499
Kall	1.31	0.086	0.33	0.32	1.00	1.0	0.4	710	1277	500	523
Merzenhausen	1.39	0.039	0.19	0.16	0.98	3.6	1.3	808	1217	458	492
Merzenhausen	1.27	0.035	0.27	0.24	0.98	3.6	1.3	719	1198	470	496
Merzenhausen	1.34	0.037	0.12	0.12	0.98	3.6	1.3	865	1197	426	466
Rollesbroich	1.09	0.068	0.46	0.48	1.00	0.6	0.2	618	1218	483	498
RollesbroichN	1.09	0.072	0.56	0.58	1.01	0.7	0.3	535	1100	442	453
RurAue	1.11	0.046	0.28	0.29	1.04	4.9	2.5	673	1166	470	491
RurAue	1.12	0.047	0.35	0.35	1.04	4.9	2.5	634	1165	479	496
Wildenrath	1.21	0.027	0.14	0.14	1.07	29.1	16.3	735	1066	543	564
Wildenrath	1.15	0.026	0.19	0.19	1.07	29.1	16.3	661	1038	553	565
Wuestebach	0.83	0.067	0.35	0.50	0.90	53.2	30.0	428	848	633	602
Temp. CRP					1.19						

[*Franz et al*., 2013c]. Therefore, *Franz et al*. [2013c] proposed an additional correction factor (CBWE) which has to be multiplied with corrected neutron intensity to relate the moderation efficiency of water located in discrete objects (i.e., tree trunks) to an equivalent layer of water. One method to determine CBWE is to model trunk size, distribution, and volume of trees in the CRP footprint using a neutron interaction model. Alternatively, N_S can be treated as a calibration parameter that includes the effect of all hydrogen pools and an appropriate value of N_S can be estimated from measured corrected neutron intensity at the time of calibration.

2.3. Quantification of Surface and Subsurface Parameters

2.3.1. CRP Calibration With In Situ Soil Sampling

Soil samples for calibration of the permanent CRPs were taken with a HUMAX soil corer (Martin Burch AG, Rothenburg, Switzerland; dimensions: 300 mm in length, 50 mm in diameter), following the COSMOS sampling scheme described earlier. Each soil core was split into six segments of 5 cm length and subsequently dried in the oven at 105°C for 48 h. This resulted in 108 samples for which the gravimetric soil water content, dry soil bulk density, and volumetric soil water content were determined from the wet and dry weight and the known sample volume. Lattice water was determined through combustion of 15 mg aliquots of dried, grinded, and 2 mm sieved soil at 1000°C using a heat conductivity detector. Lattice water in the present study includes hydrogen from organic and inorganic compounds. Root biomass was not considered in this study because measurements of root biomass are difficult to make and subject to large uncertainty. In addition, hydrogen of root biomass contributes only to a small degree to the total hydrogen pools within a CRP footprint [*Bogena et al*., 2013]. Neutron intensity was averaged over a 12 h time window at the time of calibration to determine N_0, N_{COSMIC}, and N_S from the sampling results (see Table 2).

2.3.2. CRP Calibration With SoilNet Data

Temporary CRP measurements were made at several locations in the deforested area of the Wüstebach catchment (see Figure 1). These temporary CRP measurements were calibrated using the mean soil water content determined from SoilNet for each time period and measurement location, the mean dry bulk density of the A and B horizon determined from soil samples at each SoilNet location [*Bogena et al*., 2014], and the mean lattice water content determined by *Bogena et al*. [2013] for this catchment (see Table 3). For this, SoilNet data were averaged to obtain hourly values. Periods with snow and soil temperatures below 0°C were not considered and soil water content measurements with unrealistic values (<0 cm^3 cm^{-3} or >1 cm^3 cm^{-3}) were excluded from the analysis. After adding lattice water to the volumetric soil water content measured by SoilNet, the mean vertically weighted total soil water content was calculated for each SoilNet node using the method described in *Bogena et al*. [2013]. For each individual calibration for a particular time period and CRP measurement location, a variogram was estimated based on temporally averaged

Table 3. Measurement and Calibration Results of the 13 Temporary CRP Locations (Measurement Hours (nr), Dry Soil Bulk Density (ρ_{bd}), Total Gravimetric Soil Water Content (θ_{grav}), Biomass Water Equivalent (BWE), Dry Aboveground Biomass (AGB_{dry}), Neutron Intensity (N_{epih}), Vegetation-Corrected Neutron Intensity (N_{epihv}), the N_0 Calibration Parameter, N_{COSMIC} for Not Vegetation and Vegetation-Corrected Neutron Intensity, and Calibration Parameters $N_{S,a}$ [after *Franz et al.*, 2013b] and $N_{S,b}$ [after *McJannet et al.*, 2014]

id	nr (h)	ρ_{bd} (g g^{-1})	θ_{grav} (g g^{-1})	BWE (kg m^{-2})	AGB_{dry} (kg m^{-2})	N_{epih} (cph)	N_{epihv} (cph)	N_0 (cph)	$N_{COSMIC,1}$ (cph)	$N_{COSMIC,2}$ (cph)	$N_{S,a}$ (cph)	$N_{S,a}$ (cph)
1	72	0.90	0.56	51.5	29.1	420	574	854	152	207	633	600
2	191	0.85	0.63	47.4	26.7	419	556	872	156	207	624	593
3	98	0.83	0.65	36.9	20.8	447	553	936	168	208	603	580
4	94	0.83	0.69	28.5	16.1	491	577	1039	186	219	610	593
5	27	0.83	0.76	22.8	12.9	516	585	1111	200	227	611	598
6	24	0.80	0.69	16.0	9.0	517	564	1094	197	215	548	543
7	47	0.79	0.83	14.8	8.3	469	508	1025	185	201	509	503
8	405	0.82	0.71	15.5	8.7	531	578	1129	203	221	563	558
9	129	0.81	0.76	15.8	8.9	493	537	1060	191	208	532	526
10	112	0.88	0.45	50.3	28.4	434	588	840	148	200	609	583
11	190	0.83	0.65	22.6	12.8	490	556	1027	184	209	559	550
12	190	0.82	0.64	23.3	13.1	478	544	998	179	203	547	538
13	190	0.81	0.71	13.8	7.8	501	540	1065	192	206	518	515

vertically weighted total soil water content at each SoilNet node. This variogram served to interpolate soil water content on a grid with 1 m resolution using ordinary kriging. The mean total soil water content for the CRP footprint was then obtained by averaging 360 interpolated total soil water content values at the three radii from the COSMOS sampling scheme (25, 75, and 175 m).

2.3.3. Quantification of Aboveground Biomass

Aboveground biomass was estimated from biomass samples and land use maps at the permanent CRP locations. On 18 and 19 July 2013, 18 aboveground biomass samples were taken at the permanent CRP locations, Aachen, Merzenhausen, and Gevenich, with a clipper size of 20 by 20 cm. This resulted in samples of several different crop types (e.g., winter wheat, sugar beet, rape, maize, and potato with 30, 9, 4, 3, and 1 sample each, respectively) and grassland (seven samples). These samples were weighted and dried individually at 105°C in a ventilated oven during 48 h to determine dry aboveground biomass according to the ASTM E-1756 standard [*ASTM Standard E1756-08*, 2008]. The vegetation water content was estimated from the weight loss after drying. Total biomass water equivalent consists of vegetation water as well as hydrogen and oxygen present in other molecules within the dry aboveground biomass. Here we assume that this water equivalent in dry aboveground biomass can be approximated by the amount of hydrogen and oxygen contained in cellulose ($C_6H_{10}O_5$), i.e., ~55.6% by weight. The aboveground biomass samples taken in the cropland and grassland of these three sites are assumed to be representative for all grassland and cropland in the Rur catchment. In addition, dry aboveground biomass of forest in the Rur catchment was assumed to be 18.4 kg m^{-2} [*Oehmichen et al.*, 2011] following average characteristics of coniferous and deciduous forests in Germany. We assumed that forest vegetation water content was 56% [*Nurmi*, 1999]. Land use fractions within a 300 m radius around the CRP were determined using a 15 m resolution land use map obtained from remote sensing data [*Waldhoff*, 2012]. In a final step, the mean dry aboveground biomass and mean biomass water equivalent of each CRP footprint were determined from the biomass water equivalents and dry aboveground biomass for the respective land use fractions (Table 1).

At the Wuestebach test site, aboveground forest biomass was determined directly on site by *Etmann* [2009]. Vegetation is primarily (97% by weight) cultivated Norway Spruce (*Picea abies* L.) with an age of ~65 years. Median breast height diameter was 38.0 cm with an average density of 370 trees per ha. Extensive field sampling and application of allometric functions yielded a dry aboveground forest biomass of 30 kg m^{-2} [*Etmann*, 2009], which is much higher than the average aboveground biomass of German forests due to the high planting density of this Spruce stand. The vegetation water content at the Wuestebach site was found to be between 49 and 67% of total wet aboveground biomass [*Etmann*, 2009], similar to what was found by *Nurmi* [1999].

For the deforested area at Wuestebach (Figure 1), we assumed that a small amount of aboveground biomass remained after deforestation as tree stumps, litter, and remaining or emerging vegetation (3% or AGB_{dry} = 1 kg m^{-2}). The heterogeneous distribution of aboveground biomass within the footprints of the

temporary CRPs located in the Wuestebach catchment (Figure 1) was considered using the radial segment-based weighting scheme described previously in section 2.2.2.

2.4. Analysis of Vegetation Impacts on Neutron Intensity

2.4.1. Regression of Biomass and Fast Neutron Intensity

From the calibration data set of the permanent CRPs (Table 2), a regression equation between site-specific N_0 and dry aboveground biomass or biomass water equivalent was established

$$N_0 = -r_1 \times AGB_{dry} + N_{0,AGB=0}, \tag{7}$$

$$N_0 = -r_2 \times BWE + N_{0,BWE=0}, \tag{8}$$

where r_1 in cph per kg dry aboveground biomass per m^2 and r_2 in cph per kg of biomass water equivalent per m^2 represent the change in N_0 with aboveground biomass AGB_{dry} [kg m^{-2}] or biomass water equivalent BWE [kg m^{-2}], and $N_{0,AGB=0}$ and $N_{0,BWE=0}$ [cph] is the reference N_0 for an aboveground biomass and biomass water equivalent of 0 kg m^{-2}.

2.4.2. The Empirical Vegetation Correction for Neutron Intensity

From the ratio N_{epih} / N_0 in equation (4) we derive the more general relationship $N_{epih}/N_0 = N_{epihv}/N_{0,AGB=0}$ where N_{epihv} is the fast neutron intensity corrected for vegetation (v). In order to determine N_{epihv} directly, we substituted N_0 with equations (7) and (8). The new vegetation-corrected neutron intensity N_{epihv} is then determined with the vegetation correction factor f_{veg} using

$$N_{epihv} = N_{epih} \times f_{veg} = N_{epih} \times \left(1 - r_1 / N_{0,AGB=0} \times AGB_{dry}\right)^{-1}, \tag{9}$$

$$N_{epihv} = N_{epih} \times f_{veg} = N_{epih} \times \left(1 - r_2 / N_{0,BWE=0} \times BWE\right)^{-1}. \tag{10}$$

The implementation of the vegetation correction into equation (4) yields the relationship between neutron intensity and total gravimetric soil water content

$$\theta_{grav} = a_0 \times \left(N_{epihv}/N_{0,AGB=0} - a_1\right)^{-1} - a_2. \tag{11}$$

Equation (11) represents a direct relationship between gravimetric soil water content, biomass, and fast neutron intensity that should be valid across a wide range of soils. With knowledge on biomass variation in time and space, mean lattice water content, and the single vegetation independent calibration parameter $N_{0,AGB=0}$, it should be possible to determine soil water content directly from fast neutron intensity. It is important to realize that the relationship between volumetric water content and fast neutron intensity is more complicated because of the dependence on soil bulk density that varies considerably between sites (see Table 2). Therefore, CRP results that compare soil water content of more than one site are presented in terms of gravimetric water content in the remainder of this study. Results at a single site are presented in volumetric soil water content for ease of interpretation by the reader.

2.4.3. Evaluation of the Proposed Vegetation Correction

We evaluated the proposed vegetation correction in four different ways. In the first test case, the predictions by equations (7) and (8) were compared with results from the temporary CRP measurements at the Wuestebach test site (Figure 1). The measurements were made along a steep biomass gradient, which required horizontal weighting to obtain mean aboveground biomass in the CRP footprints as described in section 2.3.3. Average soil water content was than determined as described in section 2.3.2. Using mean neutron intensity and total soil water content over the measurement period, N_0 was determined using equation (4) and compared to the predicted N_0 from the regression equations (equations (7) and (8)).

Second, we tested the vegetation correction (equation (7)) for a case where an abrupt change in aboveground biomass occurred (i.e., a deforestation experiment). For this, the permanent Wuestebach CRP was calibrated using gravimetric sampling in 2012. The resulting soil water content estimates were already compared to in situ soil water content measurements from the SoilNet by *Baatz et al.* [2014]. After the deforestation, both the measured neutron intensity and the site-specific N_0 are expected to increase due to the removal of hydrogen contained in vegetation from the CRP footprint. Therefore, we used the relative change in dry aboveground biomass to determine a new site-specific N_0 from the previously in situ determined N_0 using equation (7). From 3 April 2014 to 27 May 2014, daily soil water content estimates derived

from CRP measurements using the N_0 of the 2012 calibration campaign and the vegetation-corrected N_0 were then compared to in situ soil water content measurements from SoilNet.

In the third case, we compared in situ SoilNet measurements of soil water content at locations with low, intermediate, and high biomass with soil water content predictions obtained from CRP using efficiency and vegetation-corrected neutron intensity measurements and a single $N_{0,AGB=0}$ (equation (11)). The Rollesbroich test site is permanent grassland and represents the low biomass case. The Wuestebach test site before deforestation represents the high biomass case. For both sites, daily mean soil water content estimates derived from SoilNet and CRP were compared for 2012. These two sites were already used by *Baatz et al*. [2014] for evaluation of the CRP measurements. The difference in this study is that the neutron intensity is corrected for counting efficiency and vegetation, and that a single $N_{0,AGB=0}$ is used to estimate soil water content (equation (11)). For the intermediate biomass case, daily SoilNet data were compared with soil water content estimates derived from the permanent CRP measurements at the Wuestebach test site after the deforestation for the period from April to May 2014.

In the fourth and final test case, the COSMIC operator and the hmf method were used. The COSMIC operator is much more complex in architecture than the N_0 method. The calibration parameter of the COSMIC operator N_{COSMIC} was determined for every CRP station in the Rur catchment using neutron intensity data with and without a vegetation correction. The standard deviation of N_{COSMIC} was then used to test the efficiency of the vegetation correction in reducing variability of the site-specific N_{COSMIC} parameter. The same was done for the hmf method, keeping in mind that vegetation is considered in the hmf method (equation (5)). The N_S calibration parameter was determined from measured corrected neutron intensity with and without the empirical vegetation correction. When calibrating N_S using vegetation-corrected neutron intensity N_{epihv}, vegetation ($C_6H_{12}O_5$ and H_2O) was removed from the estimation of the hydrogen molar fraction (equation (5)) because we assume that the vegetation correction also removes the vegetation signature in measured neutron intensity.

3. Results

3.1. Calibration Campaigns and Vegetation Estimates

Mean soil parameters for the different calibration campaigns are presented in Table 2. Bulk density was lowest at the Wuestebach test site (ρ_{bd} = 0.83 g cm^{-3}) and highest at the Gevenich test site (ρ_{bd} = 1.42 g cm^{-3}). Lattice water content ranged from 0.03 to 0.09 cm^3 cm^{-3}, volumetric water content from 0.12 to 0.56 cm^3 cm^{-3}, and gravimetric soil water content ranged from 0.12 to 0.58 g g^{-1}.

Mean dry aboveground biomass of cropland and grassland were 1.61 and 0.27 kg m^{-2}, respectively, whereas the associated mean biomass water equivalent was 4.46 and 0.64 kg m^{-2}. These mean values compare well with other measurements in the Rur catchment during the same time of the year [*Korres et al*., 2013]. After consideration of the land use fractions, the mean dry aboveground biomass within the footprint of the 10 CRP stations ranged from 0.2 to 30 kg m^{-2}, or between 0.6 and 53.2 kg m^{-2} in terms of total biomass water equivalent (Table 2).

3.2. Sensor-Specific Efficiency Correction

Sensor-specific counting efficiencies for all 10 CRPs ranged from 0.90 to 1.19 (Table 2). This large variation in counting efficiency indicates a significant sensor-to-sensor variability for the CRP probe type used in this study. To test our efficiency correction approach, we compared fast neutron intensity measurements of the permanent Wuestebach station (lowest counting efficiency) with data from a nearby temporary measurement location (<5 m) with a CRP that showed the highest counting efficiency. The uncorrected neutron intensity measurements of both CRPs show considerable differences in magnitude (Figure 2). After application of the efficiency correction, this offset has been removed, which demonstrates the effectiveness of this simple correction approach (Figure 2).

3.3. Vegetation Correction

We used data from the 16 in situ soil sampling campaigns (Table 2) to determine site-specific N_0 values according to the approach of *Baatz et al*. [2014]. The lowest N_0 value was found for the permanent CRP at the Wuestebach site (forest, N_0 = 848 cph), and the largest value was found for the CRP at the Kall site (grassland, N_0 = 1277 cph). These N_0 values show a strong correlation to dry aboveground biomass

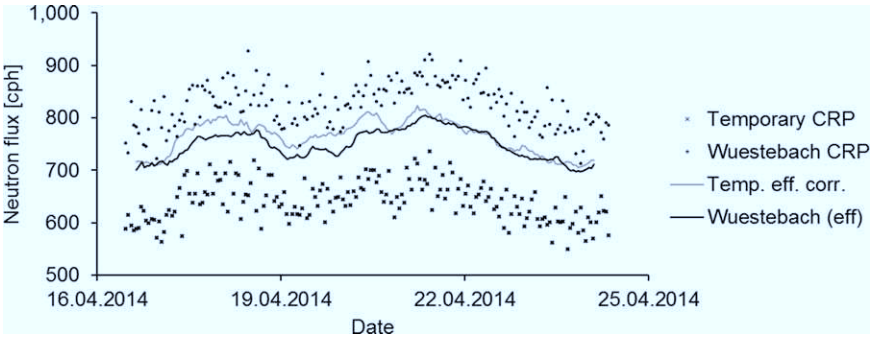

Figure 2. Parallel neutron flux measurements of the permanent Wuestebach CRP ($\eta_{Iref} = 0.90$) and a temporary CRP ($\eta_{Iref} = 1.19$) placed next to the Wuestebach CRP for testing the efficiency correction. Hourly raw neutron flux measurements are shown as points. Ten hour running mean efficiency corrected neutron flux for both CRPs are shown as lines.

($R^2 = 0.87$, Figure 3) and biomass water equivalent ($R^2 = 0.86$). Therefore, we used a linear regression to estimate N_0 as function of dry aboveground biomass (equation (7)). We found $r_1 = 11.2$ cph per kg of dry aboveground biomass per m^2 (i.e., a decrease of N_0) and the intersection with the y axis at $N_{0,AGB=0} = 1210$ cph (i.e., for 0 kg m^{-2} aboveground biomass). For BWE, we found $r_2 = 6.4$ cph per kg of BWE per m^2 and $N_{0,BWE=0} = 1215$ cph. For the more generalized form of the vegetation correction or reference conditions different than ours (efficiency, pressure, incoming cosmic ray intensity, air humidity, and cutoff rigidity), we found a neutron intensity reduction by $r_1/N_{0,AGB=0} = 0.9$ % per kg of dry aboveground biomass or $r_2/N_{0,AGB=0} = 0.5$ % per kg of biomass water equivalent (equations (9) and (10)).

3.4. Evaluation of Biomass Correction at the Wuestebach Test Site

The temporary CRP measurement locations at the Wuestebach test site (Figure 1) were selected to cover a wide range of dry aboveground biomass. The aboveground biomass for every 5 m segments for each of the 13 temporary CRP locations is shown in Figure 4. It can be seen that CRPs located in the center of the deforested area showed low aboveground biomass at small distances to the CRP station, but biomass progressively increased with increasing distance. Even CRP stations located in the center of the deforested area were only 200 m away from the large amount of aboveground biomass in the nearby forest. CRP stations located in the forest show a decreasing aboveground biomass with increasing radius to the CRP. Weighted biomass of those stations is relatively high with $AGB_{dry} \geq 20.8$ kg m^{-2}. After applying the horizontal weighting function (also see Figure 4) to these biomass distributions, we obtained weighted mean dry aboveground biomass ranging from 7.7 to 29.1 kg m^{-2} for the temporary CRP stations.

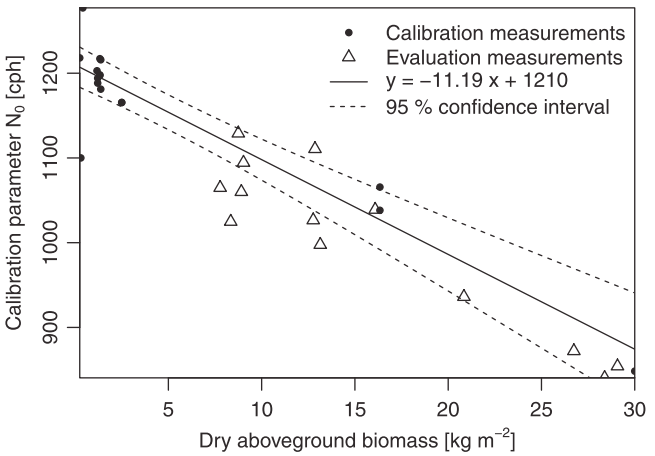

Figure 3. Calibration parameter N_0 in relation to aboveground biomass for the 16 field calibrations from *Baatz et al.* [2014] with sensor-specific efficiency correction included (dots), the regression of N_0 to dry aboveground biomass (black line), and 95% confidence interval, and the Wuestebach calibration parameters (triangles). Intercept and slope are 1210 and 11.18 cph/kg of dry aboveground biomass per m^2, respectively, $R^2 = 0.866$ and $p = 1.702e\text{-}07$.

As expected, measured neutron intensity (N_{epih}) was lowest in the forested part of the Wuestebach catchment (367 cph) and highest in the deforested area (464 cph) during the calibration period of the temporary CRP measurements. Mean total volumetric soil water content for calibration of the temporary CRPs ranged from 0.39 to 0.65 cm^3 cm^{-3}, and total gravimetric soil water content ranged between 0.44 and 0.82 g g^{-1}. The derived N_0 for the temporary CRP measurements decreased from 1129 cph for the deforested area to 840

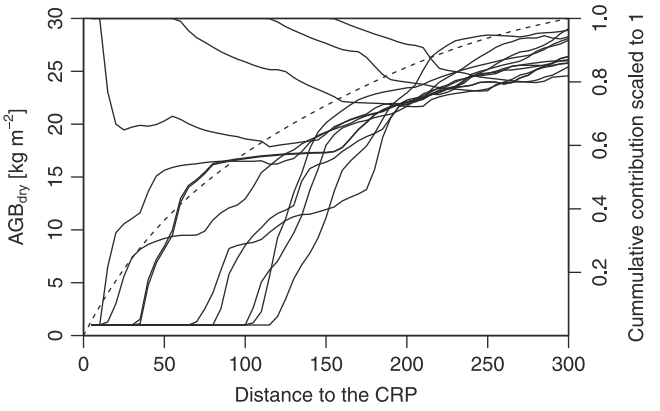

Figure 4. Aboveground biomass estimates for radial segments of the temporary CRPs at Wuestebach using the horizontal weighting scheme of *Bogena et al.* [2013] with 5 m steps. The dashed line shows the cumulative contribution of the segments to a total of 1.

cph for the forested area (Figure 3). The evaluation data confirm the clear trend of a reduction in N_0 with increasing aboveground biomass and were close to the regression line derived from the soil sampling calibration data set (Root Mean Squared Error (RMSE) = 47 cph). Overall, these measurements strongly support the relationship between N_0 and dry aboveground biomass that was presented earlier.

3.5. Evaluation of Vegetation Correction in Case of an Abrupt Change in Biomass

The second evaluation of the vegetation correction uses data from the Wuestebach test site under forested (in 2012) and deforested (in 2014) conditions. The Wuestebach CRP was calibrated in 2012 with in situ soil samples (Table 2) and we found N_0 = 848 cph and an RMSE of 0.03 cm^3 cm^{-3} between soil water content estimates from CRP and SoilNet. After the deforestation, the corrected neutron intensity (N_{epih}) showed a strong increase (Figure 5), as expected from the decrease in biomass. Soil water content estimates with the previously obtained N_0 resulted in an underestimation of soil water content in 2014 and a high offset (RMSE = 0.29 cm^3 cm^{-3}). Using the previously derived vegetation correction, we found a new N_0 = 1037 cph for a vegetation reduction from 30 to 13.1 kg m^{-2}. The accuracy of the soil water content estimates using the corrected N_0 was close to the accuracy achieved in 2012 before deforestation (RMSE = 0.03 cm^3 cm^{-3}).

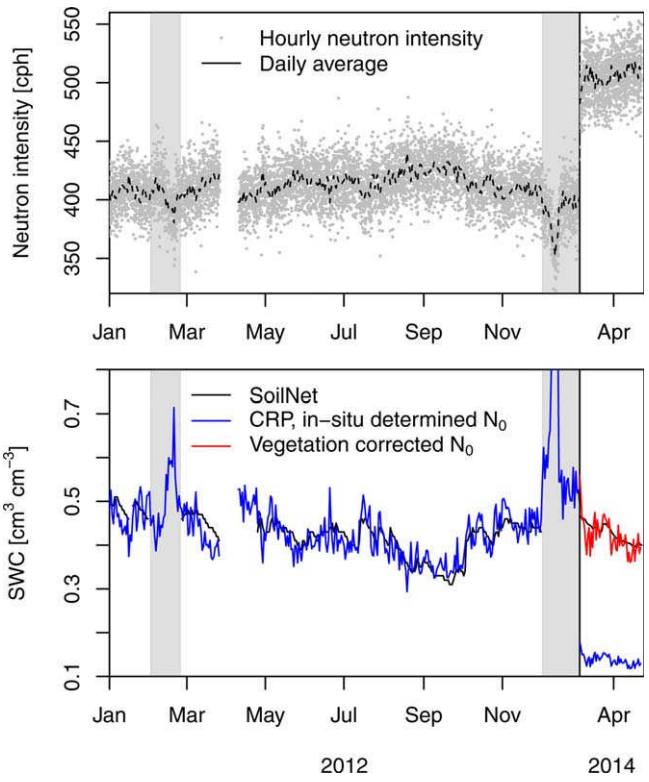

Figure 5. Measured corrected neutron intensity (N_{epih}) from the Wuestebach CRP, hourly (gray dots), and daily averaged (dashed). The lower figure shows daily volumetric soil water content estimated with the calibrated site-specific N_0 (blue) and with the N_0 estimated from the vegetation correction function (red) under deforested conditions. The black line represents horizontally and vertically weighted soil water content measured with SoilNet. Gray shaded areas indicate periods with snow.

3.6. Evaluation of Vegetation-Corrected Neutron Intensity N_{epihv} at Multiple Sites

The third evaluation of the vegetation correction compares soil water content derived with efficiency and vegetation-corrected neutron intensity (N_{epihv}) and a single $N_{0,AGB=0}$=1210 cph for three sites with different aboveground biomass to independent SoilNet measurements. The estimated dry aboveground biomass at Rollesbroich was AGB_{dry} = 0.25 kg m^{-2}. At Wuestebach, dry aboveground biomass was estimated to be 30 kg m^{-2} before deforestation and 13.1 kg m^{-2} after deforestation. Hence, the vegetation correction (equation (9)) was highest for the CRP station located in the forest of the Wuestebach catchment

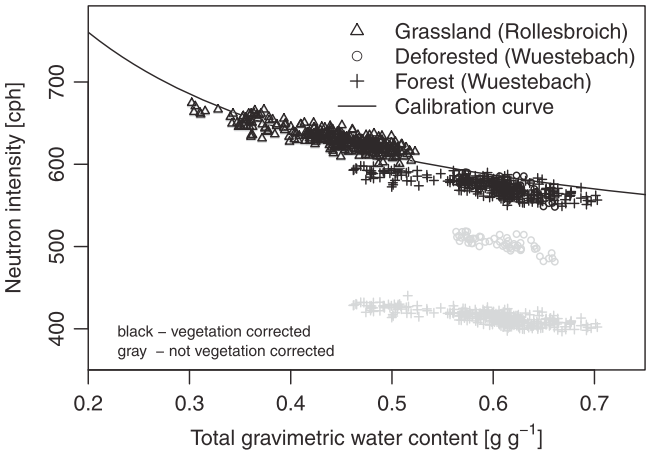

Figure 6. Daily average measured total gravimetric water content by SoilNet, not vegetation-corrected (gray, N_{epih}) and vegetation-corrected neutron intensity (black, N_{epihv}) at the permanent CRP locations Rollesbroich and Wuestebach in 2012 and 2014. The black line represents the calibration curve with $N_{0,AGB=0} = 1210$ cph to estimate soil water content from vegetation-corrected neutron intensity.

($f_{veg} = 1.38$), intermediate for the CRP station located in the deforested area ($f_{veg} = 1.14$), and lowest for the grassland test site Rollesbroich ($f_{veg} = 1.002$). Figure 6 summarizes the three independent daily averaged time series of total gravimetric soil water content generated from horizontally and vertically weighted SoilNet measurements and fast neutron intensity measurements from the permanent CRPs with (N_{epihv}) and without correction (N_{epih}). The gray markers indicate neutron intensity measurements without vegetation correction. The vegetation correction shifted the count rates observed at all sites toward the previously derived calibration curve for $N_{0,AGB=0} = 1210$ cph by the factor f_{veg}. Ideally, all measurements should fall together on the single calibration curve. Indeed, the fully corrected neutron intensity data are closely grouped and coincide with the neutron intensity—soil water content conversion derived earlier for the Rur catchment (equation (11), $N_{0,AGB=0} = 1210$ cph). Overall, the RMSE between gravimetric soil water content determined from CRP measurements and the reference gravimetric soil water content derived using SoilNet was 0.076 g g^{-1}. In terms of volumetric soil water content, the RMSE was 0.066 cm^3 cm^{-3}.

3.7. Indirect Evaluation of the Vegetation Correction

In a fourth indirect evaluation of our method, we compared the standard deviation of the COSMIC calibration parameter N_{COSMIC} for calibrations with and without vegetation-corrected neutron intensity. The standard deviation of N_{COSMIC} for the case without vegetation correction was 20 cph with a mean N_{COSMIC} of 187 cph. For this case, N_{COSMIC} showed a strong correlation with dry aboveground biomass and biomass water equivalent ($R^2 = 0.80$, Figure 7). If vegetation-corrected neutron intensity N_{epihv} was used for COSMIC calibration, the resulting N_{COSMIC} calibration parameters had a reduced standard deviation of 9 cph and a mean $N_{COSMIC} = 206$ cph. Furthermore, correlation of N_{COSMIC} with aboveground biomass was strongly reduced ($R^2 = 0.01$). Our findings agree with *Shuttleworth et al.* [2013], who suggested that a large part of the N_{COSMIC} variability among different sites may be explained by variation in aboveground biomass among calibration sites.

We also tested the hydrogen molar fraction method (hmf method) [*Franz et al.*, 2013b] with the complete calibration data set. After correction for sensor-specific counting efficiency, the calibration parameter N_S was determined with N_{epih} (Tables 2 and 3) for the parameters in equation (6) introduced by *Franz et al.* [2013b] and *McJannet et al.* [2014]. As in an earlier study made in the Rur catchment [*Baatz et al.*, 2014], we found that the calibration parameter N_S correlated with aboveground biomass with $R^2 = 0.92$ and $R^2 = 0.89$ for the parameterizations of *Franz et al.* [2013b] and *McJannet et al.* [2014], respectively. The standard deviation of N_S was 64 and 44 cph, respectively. This strong correlation confirms that an additional hmf-specific correction factor (CBWE) is required by the hmf method [*Franz et al.*, 2013c]. After application of the vegetation correction (equation (9)) to neutron intensity, the standard deviation of N_S decreased to 21 and 17 cph for both parameterizations, respectively. The newly calculated hydrogen molar fraction without vegetation was then able to explain the variation of fast neutron intensity at each location for both parameterizations to a satisfactory degree with $R^2 = 0.91$ and $R^2 = 0.86$, respectively. These results indicate that the empirical vegetation correction method is also able to enhance the hmf method.

3.8. Sensitivity of Fast Neutron Intensity to Aboveground Biomass

Using the relationship between soil water content and vegetation-corrected neutron intensity (equation (11)), a sensitivity analysis was conducted to determine how soil water content predictions (equation (4))

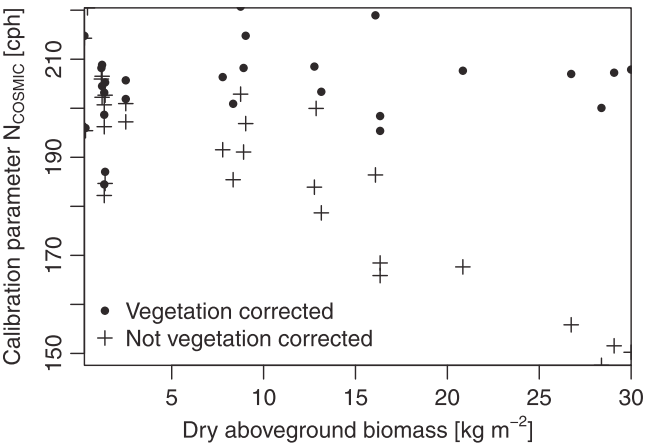

Figure 7. The COSMIC calibration parameter N_{COSMIC} without (N_{epih}, $\sigma = 20$ cph) and with vegetation-corrected neutron intensity (N_{epihv}, $\sigma = 9$ cph).

are affected by aboveground biomass. Figure 8 presents the calibration functions for four different amounts of dry aboveground biomass (0, 1.5, 15, and 30 kg m^{-2}). The curves deviate from the reference calibration curve $N_{0,AGB=0} =$ 1210 cph due to enhanced neutron moderation by additional hydrogen contained in the vegetation (equation (11)). Soil water content estimates from CRP measurements are more affected by vegetation if soil water content is high, as illustrated by the triangles in Figure 8. For example, suppose that a CRP was calibrated at point A with $\theta_{grav} =$ 0.14 g g^{-1} and neutron intensity equaled 833 cph. We assume an increase in dry aboveground biomass from 0 to 15 kg m^{-2} (surely an extreme case). If the next neutron intensity measured would be 718 cph, neglecting the change in aboveground biomass would result in a wrong soil water content estimate of $\theta_{grav} = 0.25$ g g^{-1}, at point C. Instead, the true soil water content is much lower $\theta_{grav} = 0.14$ g g^{-1}. Repeating this experiment for higher soil water content would increase this offset. In many agricultural sites, much smaller changes in aboveground biomass are expected (e.g., up to 1.5 kg m^{-2}) due to growing crops. Using the calibration functions of $AGB_{dry} = 0$ kg m^{-2} and $AGB_{dry} = 1.5$ kg m^{-2} in Figure 8, it is possible to estimate the error introduced by neglecting this change in agricultural biomass. For low gravimetric soil water content of 0.1 g g^{-1}, the error is small with 0.006 g g^{-1}. For higher soil water content, the error increases to, e.g., 0.025 g g^{-1}, for a soil water content of 0.4 g g^{-1}.

4. Discussion

The major advance in this study is the representation of neutron intensity variability by a single relationship between soil water content and vegetation-corrected neutron intensity. In particular, our measurements are well described by a single $N_{0,AGB=0}$ calibration function that explains 95% of the observed vegetation-corrected neutron intensity variability by soil water content variation for all sites analyzed in the Rur catchment (Figure 9). The remaining 5% unexplained variability may be related to interannual changes in biomass, vegetation water content, the uncertainty of the empirical parameters in the vegetation correction, as well as uncertainties in the soil water content and biomass estimation. In addition, strong spatial clustering of biomass in the CRP footprint might affect the relationship between CRP measurements and biomass [*Franz et al.*, 2013c]. Finally, root zone biomass has not been considered in our study. In forest systems this hydrogen pool is temporally stable and of less significance [*Bogena et al.*, 2013]. For agricultural sites, root biomass is temporally dynamic, which might lead to additional uncertainties associated with the transferability of the vegetation correction from one site to another. If neutron intensity is not corrected for aboveground biomass, only 76% of the fast neutron intensity variability can be explained by variations in gravimetric soil water content (Figure 10).

In order to assess how uncertainty in the biomass estimates affects soil water content predictions, we assumed that the accuracy of the dry aboveground biomass estimate is 50% (Figure 10). This is a realistic value for low biomass and a rather high value for high biomass. The resulting uncertainty in uncorrected neutron intensity is shown for four cases of aboveground biomass in Figure 10 (top figure). For low biomass, the uncertainty is minor, but for large biomass the uncertainty is up to $\pm$50 neutron counts (10 kg m^{-2}) and $\pm$100 neutron counts (30 kg m^{-2}). We propagated this uncertainty using the vegetation correction on neutron intensity into our sets of calibration data (as in Tables 2 and 3). The resulting uncertainty is shown as error bars in Figure 10. Particularly for conditions with high amounts of biomass, the error bars are large.

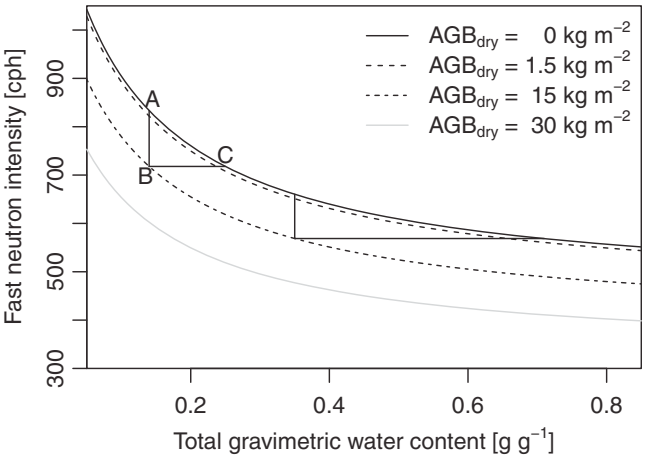

Figure 8. Sensitivity analysis of neutron intensity soil water content calibration function (equation (1)) for four cases of aboveground biomass. The four cases were calculated assuming $N_{0,AGB=0} = 1210$ cph and the proposed neutron intensity correction (equation (9)). Applying the vegetation correction on measured fast neutron intensity shifts the dashed and dotted to the solid line. As a result, the single extended N_0-method (equation (11)) could be used for soil water content estimation. If transient vegetation is not considered, the triangles illustrate how this will increasingly impact soil water content estimates from neutron intensity with increasing soil water content.

This illustrates that a substantial part of the deviation from the $N_{0,AGB=0}$ calibration curve is possibly explained by the uncertainty in the biomass estimates.

It should be noted that hydrogen is the most important neutron moderator contained in vegetation. This highlights the relevance of vegetation water content for fast neutron moderation. Especially plants with high or variable vegetation water content (e.g., maize) require consideration of total hydrogen content. In such cases, vegetation correction should be based on BWE instead of AGB_{dry}.

The obtained results in the evaluation of the proposed correction confirm that reasonable soil water content estimates can be obtained using the empirically derived vegetation correction. Because of the additional uncertainty involved in the estimation of lattice water and bulk density, we found that site-specific calibration approaches provide more accurate volumetric soil water content estimates than, e.g., regional and global calibration functions [see also *Franz et al*., 2013b]. As shown in other studies [e.g., *Franz et al*., 2013c], a combined approach of site-specific calibration and a vegetation correction for changing biomass appears to be the optimal approach for soil water content retrieval using CRPs. In future work, remote sensing of vegetation [e.g., *Butterfield and Malmstrom*, 2009; *Jackson et al*., 2004] could be a viable tool to account for transient vegetation states and to complement soil water content retrieval with CRPs [e.g., *Coopersmith et al*., 2014].

Another approach to correct fast neutron intensity for aboveground biomass was presented by *Hawdon et al*. [2014]. In contrast to the findings in this study, *Hawdon et al*. [2014] suggested a nonlinear relationship with an asymptotic behavior toward intermediate wet aboveground biomass. However, our data set shows no asymptotic behaviour for high amounts of biomass. Indeed, the relationship between fast neutron intensity and dry aboveground biomass could be weakly nonlinear, particularly for small amounts of biomass. Given the current data set, we nevertheless believe that the assumption of linearity is the most conservative one. In addition, the linear model provided a satisfactory fit to the evaluation data and required only few fitting parameters. Similar to the linear correction for absolute water vapor in air developed by *Rosolem et al*. [2013], our data set does not indicate a remarkable change in the shape of the N_0 calibration function even for high amounts of aboveground biomass.

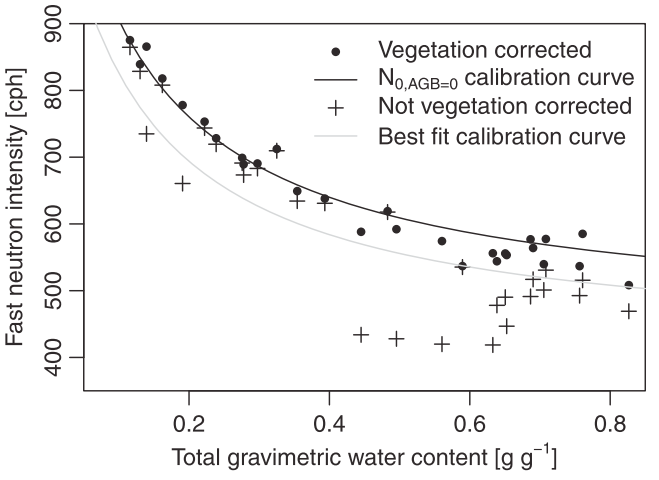

Figure 9. Neutron intensity without vegetation correction (N_{epih}, $R^2 = 0.75$) and a fitted calibration function (gray), and neutron intensity with vegetation correction (N_{epihv}, $R^2 = 0.95$) together with the extended calibration function $N_{0,AGB=0} = 1210$ cph plotted jointly for the 16 calibration measurements in the Rur catchment and the 13 evaluation measurements at the Wuestebach test site.

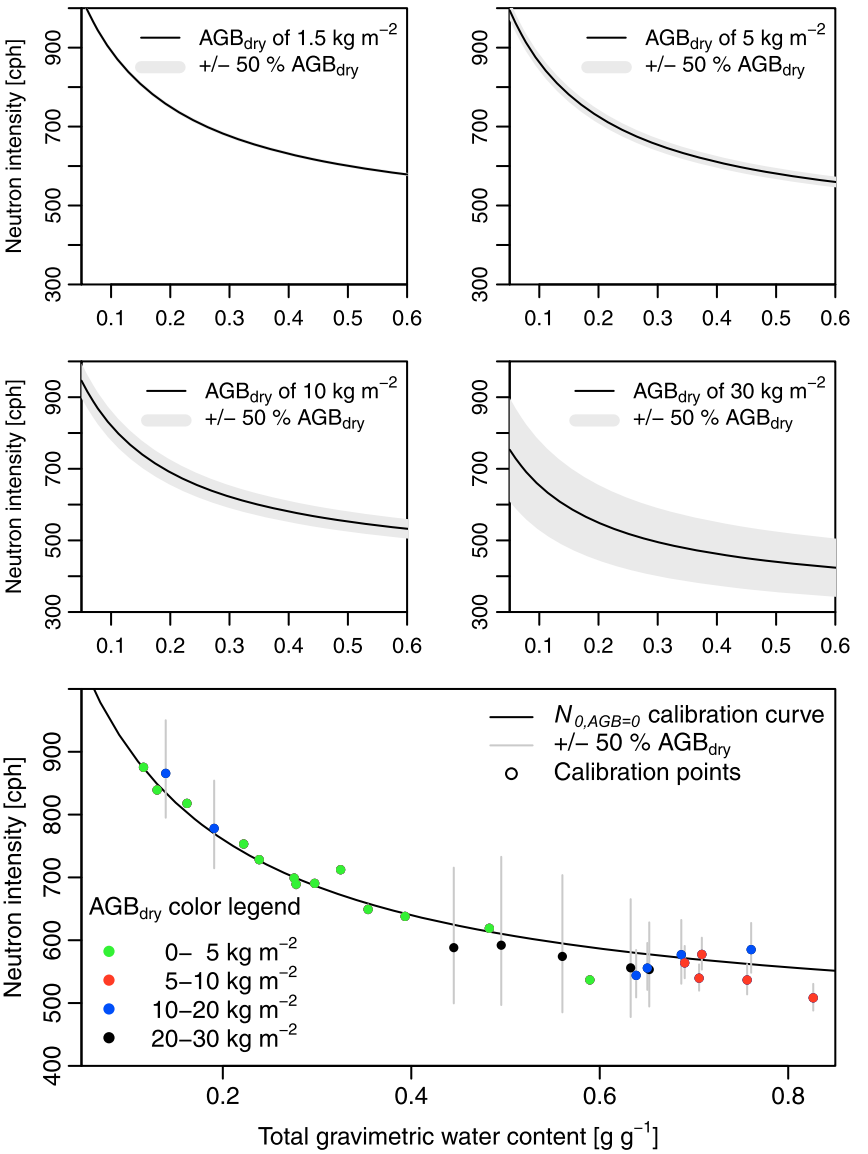

Figure 10. Uncertainty in neutron intensity assuming an uncertainty of ±50% AGB_{dry} and $N_{0,AGB=0} = 1210$ cph. The upper two figures show resulting measured fast neutron intensity N_{epih} for different biomass values, the lower figure shows the uncertainty of vegetation-corrected neutron intensity at the times of calibration based on biomass uncertainty.

The correction of neutron intensity for aboveground biomass derived in this study relies heavily on data from forest ecosystems in humid climatic conditions. Future work should investigate whether the derived relationship is also valid for other forest types (e.g., with significant undergrowth). This may not be the case because of the known effects of the geometrical distribution of biomass on measured neutron intensity [*Franz et al*., 2013c]. It seems tempting to also consider the empirical vegetation correction for correcting soil water content measurements at agricultural fields with fast changing biomass during the crop growth season. However, the derived vegetation correction has not been evaluated yet for its ability to correct for dynamical changes in agricultural biomass. Since the expected range of dynamical change in agricultural biomass is much lower than the range of biomass used to derive the vegetation correction, it has to be used with caution in this case. Furthermore, given the apparent discrepancies between our data and those of *Hawdon et al*. [2014] and with respect to the effect of small amounts of biomass (<5 kg m^{-2} AGB_{dry}) on measured neutron intensity, more research is required to address uncertainties associated with soil water content monitoring with CRP in agricultural fields. Finally, the obtained empirical relationship between the amount of aboveground biomass and N_0 should be tested for other regions of the world. This was not

possible in the context of this study because cutoff rigidities and sensor-specific counting efficiencies for installed CRPs at other locations (e.g., within the COSMOS network in North America) were not available.

5. Conclusions

We presented a new correction method that extends the capabilities of the N_0 method, the COSMIC operator and the hmf method to estimate soil water content from fast neutron intensity to sites and areas with strong spatial variation in aboveground biomass. In addition, we present a simple approach to account for sensor-specific counting efficiencies among multiple CRPs. The vegetation correction was developed using an extensive data set from a network of 10 CRPs located in the Rur catchment, Germany. An evaluation was performed using additional CRP measurements, the COSMIC operator, and the hmf method. The vegetation correction is applicable for either biomass water equivalent (BWE) or dry aboveground biomass (AGB_{dry}).

Overall, there are four main conclusions that could be drawn from this study. First, the variation in sensor-specific counting efficiency was higher than 10% among our 11 CRPs which is the same order of magnitude as the water vapor correction in humid climates [*Rosolem et al*., 2013]. Without correction of this variable counting efficiency, the subsequent analysis of the effect of aboveground biomass on the fast neutron intensity measurements would not have provided meaningful results. Second, a linear correlation was found between the calibration parameter N_0 and dry aboveground biomass or biomass water equivalent, which was successfully used to develop a vegetation correction for fast neutron intensity measurements. Third, the reduction in fast neutron intensity was quantified to be 0.9% per kg dry aboveground biomass per m^2 or 0.5% per kg of biomass water equivalent per m^2 independent of the chosen reference conditions. Finally, our results indicate that the N_0 method, the COSMIC operator and the hmf method work similarly well for the Rur catchment with the empirical vegetation correction. It is desirable to extend the results of this study to other CRP networks (e.g., COSMOS) but this would require an accurate assessment of counting efficiency of each CRP.

Acknowledgments
We gratefully acknowledge the support by the SFB-TR32 "Pattern in Soil-Vegetation-Atmosphere Systems: Monitoring, Modeling, and Data Assimilation" funded by the Deutsche Forschungsgemeinschaft (DFG) and TERENO (Terrestrial Environmental Observatories) funded by the Helmholtz-Gemeinschaft. We thank Daniel Dolfus, Martina Klein, and Bernd Schilling for supporting the ongoing maintenance of the cosmic ray stations. Most data presented in this study are freely available via the TERENO data portal TEODOOR (http://teodoor.icg.kfa-juelich.de/). We also acknowledge the NMDB database (http://www.nmdb.eu) funded by the EU-FP7, the Kiel neutron monitor operated by the Christian-Albrechts University of Kiel, and the Jungfraujoch neutron monitor operated by the University of Bern for providing data on incoming neutron flux.

References

ASTM Standard E1756-08 (2008), *ASTM E1756-08 Standard Test Method for Determination of Total Solids in Biomass*, ASTM International, West Conshohocken, Pa.
Baatz, R., H. R. Bogena, H. J. H. Franssen, J. A. Huisman, W. Qu, C. Montzka, and H. Vereecken (2014), Calibration of a catchment scale cosmic-ray probe network: A comparison of three parameterization methods, *J. Hydrol.*, *516*, 231–244.
Bogena, H. R., M. Herbst, J. A. Huisman, U. Rosenbaum, A. Weuthen, and H. Vereecken (2010), Potential of wireless sensor networks for measuring soil water content variability, *Vadose Zone J.*, *9*(4), 1002–1013.
Bogena, H. R., et al. (2012), TERENO—Ein langfristiges Beobachtungsnetzwerk für die terrestrische Umweltforschung, *Hydrol. Wasserbewirtsch.*, *3*, 138–143.
Bogena, H. R., J. A. Huisman, R. Baatz, H. J. H. Franssen, and H. Vereecken (2013), Accuracy of the cosmic-ray soil water content probe in humid forest ecosystems: The worst case scenario, *Water Resour. Res.*, *49*, 5778–5791, doi:10.1002/wrcr.20463.
Bogena, H. R., et al. (2014), A terrestrial observatory approach to the integrated investigation of the effects of deforestation on water, energy, and matter fluxes, *Sci. China Earth Sci.*, *58*, 61–75.
Brocca, L., T. Tullo, F. Melone, T. Moramarco, and R. Morbidelli (2012), Catchment scale soil moisture spatial-temporal variability, *J. Hydrol.*, *422*, 63–75.
Brutsaert, W. (2005), *Hydrology: An Introduction*, vol. xi, 605 p., Cambridge Univ. Press, Cambridge, N. Y.
Butterfield, H. S., and C. M. Malmstrom (2009), The effects of phenology on indirect measures of aboveground biomass in annual grasses, *Int. J. Remote Sens.*, *30*(12), 3133–3146.
Chrisman, B., and M. Zreda (2013), Quantifying mesoscale soil moisture with the cosmic-ray rover, *Hydrol. Earth Syst. Sci.*, *17*(12), 5097–5108.
Coopersmith, E. J., M. H. Cosh, and C. S. T. Daughtry (2014), Field-scale moisture estimates using COSMOS sensors: A validation study with temporary networks and leaf-area-indices, *J. Hydrol.*, *519*, 637–643.
Desilets, D., and M. Zreda (2003), Spatial and temporal distribution of secondary cosmic-ray nucleon intensities and applications to in situ cosmogenic dating, *Earth Planet. Sci. Lett.*, *206*(1–2), 21–42.
Desilets, D., and M. Zreda (2013), Footprint diameter for a cosmic-ray soil moisture probe: Theory and Monte Carlo simulations, *Water Resour. Res.*, *49*, 3566–3575, doi:10.1002/wrcr.20187.
Desilets, D., M. Zreda, and T. P. A. Ferre (2010), Nature's neutron probe: Land surface hydrology at an elusive scale with cosmic rays, *Water Resour. Res.*, *46*, W11505, doi:10.1029/2009WR008726.
Etmann, M. (2009), Dendrologische Aufnahmen im Wassereinzugsgebiet Oberer Wüstebach anhand verschiedener Mess- und Schätzverfahren, Diploma thesis, 91 p., Westfälische Wilhelms-Univ. Münster, Münster, Germany.
Franz, T. E., M. Zreda, R. Rosolem, and T. P. A. Ferre (2012a), Field validation of a cosmic-ray neutron sensor using a distributed sensor network, *Vadose Zone J.*, *11*(4).
Franz, T. E., M. Zreda, T. P. A. Ferre, R. Rosolem, C. Zweck, S. Stillman, X. Zeng, and W. J. Shuttleworth (2012b), Measurement depth of the cosmic ray soil moisture probe affected by hydrogen from various sources, *Water Resour. Res.*, *48*, W08515, doi:10.1029/2012WR011871.
Franz, T. E., M. Zreda, T. P. A. Ferre, and R. Rosolem (2013a), An assessment of the effect of horizontal soil moisture heterogeneity on the area-average measurement of cosmic-ray neutrons, *Water Resour. Res.*, *49*, 6450–6458, doi:10.1002/wrcr.20530.

Franz, T. E., M. Zreda, R. Rosolem, and T. P. A. Ferre (2013b), A universal calibration function for determination of soil moisture with cosmic-ray neutrons, *Hydrol. Earth Syst. Sci.*, *17*(2), 453–460.
Franz, T. E., M. Zreda, R. Rosolem, B. K. Hornbuckle, S. L. Irvin, H. Adams, T. E. Kolb, C. Zweck, and W. J. Shuttleworth (2013c), Ecosystem-scale measurements of biomass water using cosmic ray neutrons, *Geophys. Res. Lett.*, *40*, 3929–3933, doi:10.1002/grl.50791.
Hawdon, A., D. McJannet, and J. Wallace (2014), Calibration and correction procedures for cosmic-ray neutron soil moisture probes located across Australia, *Water Resour. Res.*, *50*, 5029–5043, doi:10.1002/2013WR015138.
Hendrick, L. D., and R. D. Edge (1966), Cosmic-ray neutrons near earth, *Phys. Rev.*, *145*(4), 1023.
Jackson, T. J., D. Y. Chen, M. Cosh, F. Q. Li, M. Anderson, C. Walthall, P. Doriaswamy, and E. R. Hunt (2004), Vegetation water content mapping using Landsat data derived normalized difference water index for corn and soybeans, *Remote Sens. Environ.*, *92*(4), 475–482.
Jung, M., et al. (2010), Recent decline in the global land evapotranspiration trend due to limited moisture supply, *Nature*, *467*(7318), 951–954.
Korres, W., T. G. Reichenau, and K. Schneider (2013), Patterns and scaling properties of surface soil moisture in an agricultural landscape: An ecohydrological modeling study, *J. Hydrol.*, *498*, 89–102.
Koster, R. D., et al. (2004), Regions of strong coupling between soil moisture and precipitation, *Science*, *305*(5687), 1138–1140.
McJannet, D., T. Franz, A. Hawdon, D. Boadle, B. Baker, A. Almeida, R. Silberstein, T. Lambert, and D. Desilets (2014), Field testing of the universal calibration function for determination of soil moisture with cosmic-ray neutrons, *Water Resour. Res.*, *50*, 5235–5248, doi:10.1002/2014WR015513.
Montzka, C., M. Canty, R. Kunkel, G. Menz, H. Vereecken, and F. Wendland (2008), Modelling the water balance of a mesoscale catchment basin using remotely sensed land cover data, *J. Hydrol.*, *353*(3–4), 322–334.
Nurmi, J. (1999), The storage of logging residue for fuel, *Biomass Bioenergy*, *17*(1), 41–47.
Oehmichen, K., et al. (2011), Inventurstudie 2008 und Treibhausgasinventar Wald, Johann Heinrich von Thünen-Institut Bundesforschungsinstitut für Ländliche Räume, Wald und Fischerei.
Pelowitz, D. B. (2005), MCNPX user's manual, version 5, *Rep. LA-CP-05–0369*, Los Alamos Natl. Lab., Los Alamos, N. M.
Qu, W., H. R. Bogena, J. A. Huisman, and H. Vereecken (2013), Calibration of a novel low-cost soil water content sensor based on a ring oscillator, *Vadose Zone J.*, *12(2)*.
Robinson, D. A., C. S. Campbell, J. W. Hopmans, B. K. Hornbuckle, S. B. Jones, R. Knight, F. Ogden, J. Selker, and O. Wendroth (2008), Soil moisture measurement for ecological and hydrological watershed-scale observatories: A review, *Vadose Zone J.*, *7*(1), 358–389.
Rosenbaum, U., H. R. Bogena, M. Herbst, J. A. Huisman, T. J. Peterson, A. Weuthen, A. W. Western, and H. Vereecken (2012), Seasonal and event dynamics of spatial soil moisture patterns at the small catchment scale, *Water Resour. Res.*, *48*, W10544, doi:10.1029/2011WR011518.
Rosolem, R., W. J. Shuttleworth, M. Zreda, T. E. Franz, X. Zeng, and S. A. Kurc (2013), The effect of atmospheric water vapor on neutron count in the cosmic-ray soil moisture observing system, *J. Hydrometeorol.*, *14*(5), 1659–1671.
Rosolem, R., T. Hoar, A. Arellano, J. L. Anderson, W. J. Shuttleworth, X. Zeng, and T. E. Franz (2014), Translating aboveground cosmic-ray neutron intensity to high-frequency soil moisture profiles at sub-kilometer scale, *Hydrol. Earth Syst. Sci.*, *18*(11), 4363–4379.
Shuttleworth, J., R. Rosolem, M. Zreda, and T. Franz (2013), The COsmic-ray Soil Moisture Interaction Code (COSMIC) for use in data assimilation, *Hydrol. Earth Syst. Sci.*, *17*(8), 3205–3217.
Vereecken, H., J. A. Huisman, H. Bogena, J. Vanderborght, J. A. Vrugt, and J. W. Hopmans (2008), On the value of soil moisture measurements in vadose zone hydrology: A review, *Water Resour. Res.*, *44*, W00D06, doi:10.1029/2008WR006829.
Vereecken, H., et al. (2014), On the spatio-temporal dynamics of soil moisture at the field scale, *J. Hydrol.*, *516*, 76–96.
Villarreyes, C. A. R., G. Baroni, and S. E. Oswald (2011), Integral quantification of seasonal soil moisture changes in farmland by cosmic-ray neutrons, *Hydrol. Earth Syst. Sci.*, *15*(12), 3843–3859.
Waldhoff, G. (2012), Enhanced land use classification of 2009 for the Rur catchment, TR32DB.
Zacharias, S., et al. (2011), A network of terrestrial environmental observatories in Germany, *Vadose Zone J.*, *10*(3), 955–973.
Zreda, M., D. Desilets, T. P. A. Ferre, and R. L. Scott (2008), Measuring soil moisture content non-invasively at intermediate spatial scale using cosmic-ray neutrons, *Geophys. Res. Lett.*, *35*, L21402, doi:10.1029/2008GL035655.
Zreda, M., W. J. Shuttleworth, X. Zeng, C. Zweck, D. Desilets, T. Franz, and R. Rosolem (2012), COSMOS: The cosmic-ray soil moisture observing system, *Hydrol. Earth Syst. Sci. Discuss.*, *16*, 4079–4099.